Journal of Pharmaceutical and Biomedical Analysis 209 (2021) 114482

Contents lists available at ScienceDirect

Journal of Pharmaceutical and Biomedical Analysis

journal homepage: www.elsevier.com/locate/jpba

# Molecular interactions in remdesivir-cyclodextrin systems

Bianka Várnai[a], Milo Malanga[b], Tamás Sohajda[b], Szabolcs Béni[a,*]

[a] Semmelweis University, Department of Pharmacognosy, Üllői út. 26, H-1085 Budapest, Hungary
[b] CycloLab, Cyclodextrin R&D Ltd, Illatos út 7, Budapest H-1097, Hungary

ARTICLE INFO

*Article history:*
Received 21 September 2021
Received in revised form 5 November 2021
Accepted 14 November 2021
Available online 23 November 2021

*Keywords:*
Veklury
Sulfobutylated-cyclodextrin
Complexation
NMR
Stability constant
$pK_a$ value

ABSTRACT

Remdesivir (REM) is the first antiviral drug (Veklury™) approved by the Food and Drug Administration for the therapy of COVID-19. Due to its poor water solubility, the preparation of Veklury™ requires a suitable solubilizing excipient at pH 2 conditions. For this purpose, the final formulation contains the randomly substituted sulfobutylether-β-cyclodextrin (SBEβCD) as a complexing agent. Herein, extensive NMR spectroscopic study with various cyclodextrin (CD) derivatives were conducted to understand the interactions in SBEβCD - REM systems at the molecular level. The $pK_a$ value of REM has been determined experimentally for the first time, as the protonation state of the aminopyrrolo-triazine moiety can play a key role in CD-REM inclusion complex formation as SBEβCD has permanent negative charges. The UV-pH titration experiments yielded a $pK_a$ of 3.56, thus the majority of REM bears a positive charge at pH 2.0.

NMR experiments were performed on β- and γCD derivatives to determine complex stabilities, stoichiometries and structures. The stability constants were determined by nonlinear curve fitting based on $^1$H NMR titrations at pH 2.0, while Job's method was used to determine the stoichiometries. βCD complexes were one order of magnitude more stable than their γCD counterparts. Sulfobutylation resulted in a significant increase in stability and the single isomer derivatives showed unexpectedly high stability values (log$K$ = 4.35 for REM - per-6-SBEβCD). In the case of βCDs, the ethylbutyl-moiety plays a key role in complexation immersing into the βCD cavity, while the phenoxy-moiety overtakes and drives the inclusion of REM in the case of γCDs. This is the first comprehensive study of REM-CD complexation, allowing the design of new CD derivatives with tailored stabilities, thereby aiding the formulation or production and even the analytical characterization of REM.



## 1. Introduction

In December 2019, Wuhan, China, SARS-CoV-2 (Severe Acute Respiratory Syndrome Coronavirus 2) caused an outbreak of a severe respiratory illness which was then arguably declared to be one of the most serious health concerns that has impacted the entire world [1,2]. Since the beginning of the pandemic, several investigational drugs have been explored. Among these agents, remdesivir (REM) was the first antiviral agent (Veklury™) approved by US Food and Drug Agency for the treatment of COVID-19 [3]. REM has broad antiviral activity against mRNA viruses, originally developed to treat hepatitis C and Ebola infections [4]. It is a monophosphoramidate prodrug (Fig. 1A), that is metabolically transformed into the pharmacologically active nucleoside, a triphosphate analog. The active metabolite competes with adenosine phosphate and acts as an RNA-dependent RNA polymerase inhibitor [5]. Due to REM's high first pass liver metabolism, it cannot be applied orally [6], thus an intravenous infusion in the form of a parenteral solution is the only approved administration route. REM is poorly soluble in water (0.028 mg/mL) therefore solubilizing excipients are required to formulate the product. At an early stage of the formulation a randomly substituted multicomponent mixture of sulfobutylether-beta-cyclodextrin (SBEβCD, DS ~ 6.5) is used at pH 2.0 for this purpose [7]. The permanently negatively charged SBEβCD is able to complex REM through non-covalent intermolecular interactions, thereby significantly enhances its solubility. Cyclodextrins (CDs) are cyclic oligosaccharides built of D-glucopyranose units (α-, β- and γ-CDs - six, seven and eight glucose units) linked via α-1,4-glycosidic bonds. As a result, they have a lipophilic inner cavity and a hydrophilic outer surface [8]. This particular structure enables reversible inclusion complex formation with guest molecules [9]. Synthetic modification of the hydroxyl groups of the glucopyranose units offers numerous possibilities for the preparation of various hosts for drug formulation. Fig. 1B shows the structure of the CDs included in our study. In

* Corresponding author.
*E-mail address:* beni.szabolcs@pharma.semmelweis-univ.hu (S. Béni).

https://doi.org/10.1016/j.jpba.2021.114482
0731-7085/

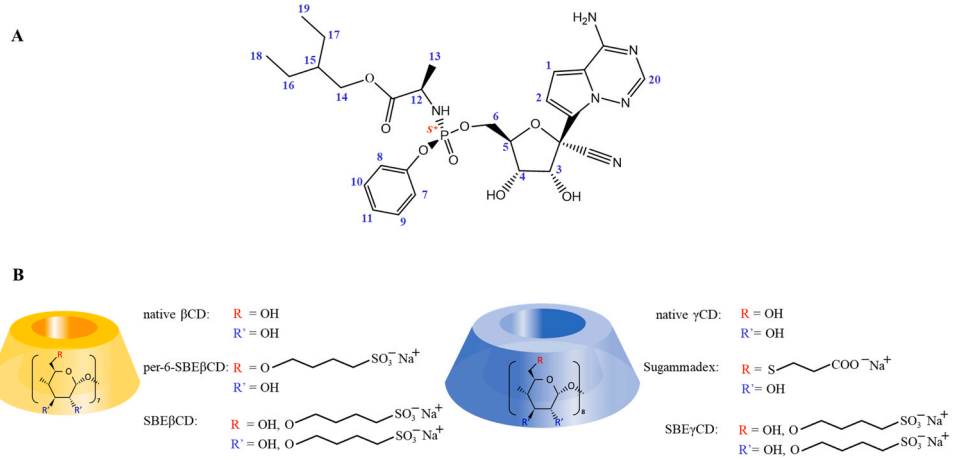


**Fig. 1.** Chemical structures and numbering of the remdesivir (**A**) and the studied β- and γ-cyclodextrin (7 and 8 glucose units) derivatives (**B**).

the present article several β- and γCD derivatives were used to characterize REM's charge-dependent molecular encapsulation. In order to understand charge-dependent behavior of REM, its experimental p$K_a$ value was also determined.

## 2. Materials and methods

### 2.1. Materials

REM was purchased from Echemi Pharma, Qingdao, China. The native βCD, the randomly substituted (SBEβCD DS ~ 6.5) and the single isomer per-6-sulfobutylated (per-6-SBEβCD DS = 7.0, [10]) βCD derivatives as well as three γCDs, native γCD, the randomly substituted SBEγCD (DS = 5.7) and the single isomer sugammadex [11] were products of CycloLab Ltd. (Budapest, Hungary). $D_2O$ (99.9 atom% D) and DMSO (≥99.7% HPLC grade) and DMSO-$d_6$ (99.9 atom% D) were purchased from Merck (Darmstadt, Germany). Other base chemicals of analytical grade were from commercial suppliers and were used without further purification.

### 2.2. UV-pH titration

500 mL stock solution was prepared by dissolving the appropriate amount of $Na_2HPO_4$ (15.0 mM) and $HCO_2NH_4$ (20 mM). The desired pH values ranging from 1.75 to 5.26 (14 individual samples) were adjusted by 6.0 M HCl and 6.0 M NaOH (pH was controlled by a Metrohm 913 pH meter combined with a standard glass electrode). Thereafter, 30 μL 15 mM REM DMSO stock solution was added to each 10 mL portion of the buffered samples at a given pH, while 30 μL of DMSO were used in case of the blank solutions. UV-Vis spectra were recorded in the 220–400 nm range on a Unicam UV2 UV/Vis Spectrometer at room temperature. The whole matrix of measured absorbances in the range of 227–345 nm (typically, 590 wavelengths at each pH values) was involved in the computer evaluation using nonlinear regression as mentioned in the literature [12] by the OPIUM program [13] to yield the p$K_a$ of REM.

### 2.3. NMR spectroscopy

Nuclear magnetic resonance (NMR) spectroscopy measurements were carried out on a 600 MHz Varian DDR NMR spectrometer (Agilent Technologies, Palo Alto, CA, USA), equipped with a 5 mm inverse-detection probehead and a gradient module. Standard pulse sequences and processing routines available in VnmrJ 3.2 C/ Chempack 5.1 and MestreNova 14.2.0 were used. The complete resonance assignments of REM and the CDs (Tables S1-2., Figs. S1-11.) were established from direct $^1H$–$^{13}C$, long-range $^1H$–$^{13}C$, and scalar spin-spin connectivities derived from 1D $^1H$, 2D $^1H$-$^1H$ gCOSY, zTOCSY (mixing time of 150 ms), ROESYAD (mixing time of 300 and 400 ms), NOESY and $^1H$–$^{13}C$ gHSQCAD ($^1J_{CH}$ = 140 Hz) experiments. The $^1H$ chemical shifts were referenced to the methyl singlet ($\delta$ = 3.31 ppm) of internal $CH_3OH$. All NMR spectra were acquired in standard 5 mm NMR tubes at 298 K.

#### 2.3.1. $^1H$ NMR titration experiments

The stoichiometry of REM complexation with various CDs was investigated by Job's method of continuous variation [14]. Samples were prepared in acidic ($D_2O$, HCl; pH 2.0) solutions at 298 K. The total molar concentration of the host and guest components $c_{REM} + c_{CD}$ was kept constant at 1 mM, while the mole fraction of REM, $x_{REM} = c_{REM} / (c_{REM} + c_{CD})$ was varied gradually in 0.1 unit steps from 0 to 1. $^1H$ chemical shifts $\delta^{REM}$ were recorded at 600 MHz for several REM resonances and complexation-induced displacement values $\Delta\delta^{REM} = |\delta^{REM} - \delta_{REM}|$ were calculated with respect to $\delta_{REM}$ measured in the absence of CD. To construct Job's plots, $\Delta\delta^{REM}$ values were multiplied by the mole fraction of REM and depicted as a function of $x_{REM}$.

To determine the apparent and averaged - in the case of the random substituted CD derivatives - stability constant in each case, separate $^1H$ NMR titrations were performed on acidic samples. For each βCD derivative 500 μL 1 mM REM was titrated with increasing portions (5–1000 μL) of CD stock solutions (10 mM βCD, 6.16 mM SBEβCD, 9.05 mM per-6-SBEβCD, 11.45 mM γCD, 6.16 mM SBEγCD) while in case of the native γCD 500 μL 0.45 mM REM was titrated with 10 mM γCD. Due to the poor solubility of sugammadex, the conditions were changed as follows: 500 μL of 0.2 mM REM solution was titrated with 5–600 μL of 0.66 mM sugammadex stock solution. Following equilibration, $^1H$ NMR spectra were recorded in each titration step at 600 MHz and 298 K. Both titration datasets were analyzed by the following method. The experimental titration curves for well-resolved resonances of REM were evaluated by the Origin software, using the 1:1 REM:CD complex as confirmed by the Job's method. If complexation occurs with rapid kinetics on the NMR chemical shift timescale, the observed chemical shift $\delta^{obs}_{REM,\,i}$ of the *i*th carbon-bound proton in REM becomes a mole-fraction weighted average of the species-specific values in the uncomplexed REM ($\delta^{REM,i}$) and in the complex ($\delta^{REM\cdot CD,i}$),

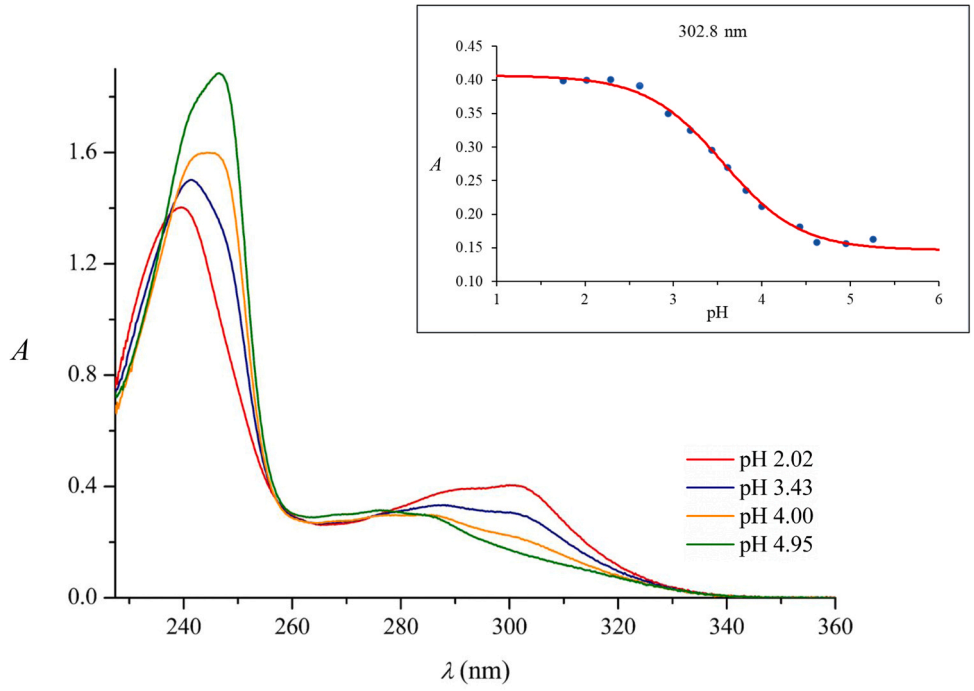


**Fig. 2.** UV absorption spectra of REM recorded at different pH values and the titration curve at 302 nm, fitted simultaneously for each registered wavelength.

$$\delta^{obs}_{REM,\,i} = \frac{\delta^{REM,\,i}\cdot c_{REM} + \delta^{REM\cdot CD,\,i}\cdot c_{REM\cdot CD}}{c^{REM}_{total}} \quad (1)$$

where $c_{CD}$ and $c_{REM}$ denote equilibrium concentrations, while $c^{CD}_{total}$ and $c^{REM}_{total}$ are the total concentrations of the compounds in the solution [15].

Chemical shifts for all hydrogens ($i$) of REM were plotted as a function of $V_{CD}$ (μL) to select the resonances with sufficient sensitivity ($\Delta\delta$) to enter the evaluation. The selected datasets were fitted to the model described above, in order to determine the apparent complex stability constant (log $K$) values.

### 2.3.2. NMR structural studies on complex formation

To explore the spatial arrangement of the host-guest complexes, nuclear Overhauser effect (NOE) type experiments [16] were performed on different molar ratio REM:CD samples under acidic conditions (pH 2.0), at 298 K. 2D ROESY spectra were acquired on the 600 MHz instrument, collecting 16 and 32 scans on 1258·512 data points, applying mixing times of 300 and 400 ms, respectively.

## 3. Results and discussion

### 3.1. Determination of REM's p$K_a$ by UV-pH titration method

Currently, there are no experimentally supported literature data on the p$K_a$ value of REM, only predicted (*in silico*) data are available [17], however, the protonation state influences its intermolecular interactions. Based on our observations, REM solubility significantly increases below pH 3.5, suggesting that protonation may occur in this region. Interestingly in reference [18], the predicted p$K_a$ value of REM (p$K_a$ 0.65) seems rather low, however the site of protonation is presumably the rare, yet basic aminopyrrolo-triazin moiety. As the aminopyrrolo-triazin part is the strongest chromophore of REM, the protonation of REM evokes an intense pH-dependent spectral shift. Consequently, UV-pH titration could be the first choice to provide a reliable p$K_a$ value. Fig. 2 shows the registered UV absorption spectra of REM at various pH values. Acidifying the solution results in hypochromic and hypsochromic effects in the range of 240–250 nm, while hyperchromic and bathochromic effects could be observed in the range of 280–320 nm. The largest changes in the absorbance values were observed at ~245 and ~303 nm. To determine the exact p$K_a$ value, the whole matrix of measured absorbances was involved in the evaluation, titration curves were fitted simultaneously for all wavelengths (see inset of Fig. 2). This evaluation yielded a p$K_a$ = 3.56 with an estimated standard deviation of 0.01. Therefore, at least 97% of REM molecules are present in monoprotonated form under pH 2.0 conditions.

### 3.2. Cyclodextrin complex stabilities of REM

The complex stoichiometry and stability for all six CD-REM systems were assessed by NMR spectroscopy. The complete resonance assignments of REM can be found in Supporting Information Table S1. The most sensitive (showing the largest complexation induced chemical shift changes), non-overlapping and well-separated $^1$H NMR resonances of REM were observed in each case. In the case of βCD, Job's plot curves (Supporting Information Fig. S12) show a maximum at x = 0.5, suggesting the formation of 1:1 complex stoichiometry. Similarly, Job's experiments were performed with the other CD derivatives (data not shown) confirming identical averaged stoichiometry.

To determine the stability constants of CD-REM complexes, single-tube $^1$H NMR titrations were carried out in all cases. During the titration of REM with βCD, chemical shift variation of the following REM resonances was monitored: H1, H2, H7–8, H9–10, H11, H13, H15, H18–19 (Fig. 3A). In order to extract a robust and reliable

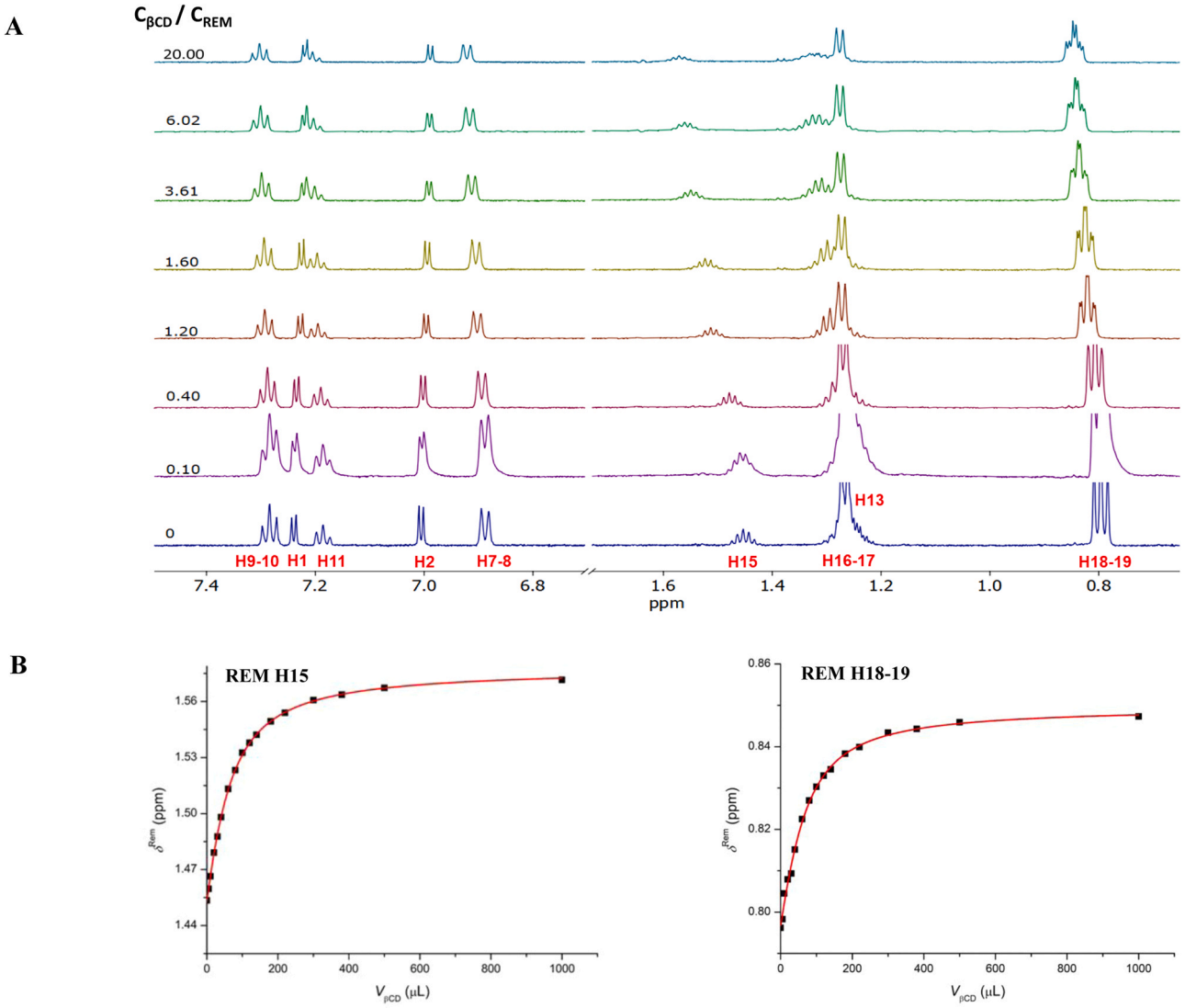


**Fig. 3.** Representative $^{1}$H NMR chemical shift changes of REM (subplot A) upon titration with βCD. Subplot B shows the selected titration profiles of REM H18–19 and H15, simultaneously fitted by the 1:1 complexation model using Origin program.

stability constant [19], all eight datasets were subjected to a simultaneous nonlinear regression using Origin software (Fig. 3B). This global evaluation yielded a log*K* = 3.06 with an estimated standard deviation of 0.01, a strong binding affinity for βCD. All the other chemical shift changes are depicted in Supporting Information Figs. S13–17., while the obtained stability values are summarized in Table 1. Comparing the native CDs, a tenfold decrease in stability could be observed when using γCD. Generally, the introduction of the anionic sulfobutylether-sidechains on the CD hosts contribute to a significant stability enhancement (more than fivefold for γCD, while tenfold increase for βCD, respectively), resulting in a high affinity system for REM and SBEβCD (averaged and apparent log*K* = 3.99) [20]. It has also been revealed that the number of the anionic sidechains located on the primary side of the host plays a critical role in the stability of the inclusion complex. The single isomer sulfobutylether-CD (per-6-SBEβCD) results in an additional two-fold increase in stability with the monoprotonated REM compared to the random SBEβCD, owing to the seven anionic sidechains located on the primary side of the host. Sugammadex is almost fully protonated under pH 2.0 conditions (in-house data) and possesses shorter sidechains than the sulfobutylether-CD derivatives, therefore limited electrostatic interactions can occur between the host and REM. The

**Table 1**
Stability constant values of the investigated CD-REM complexes, determined by Origin software.

| | βCD | γCD | SBEβCD (DS ~ 6.5) | per6-SBEβCD (DS = 7.0) | sugammadex (DS = 8.0) | SBEγCD (DS ~ 5.7) |
|---|---|---|---|---|---|---|
| **log*K*** | 3.06 ± 0.01 | 2.08 ± 0.02 | 3.99 ± 0.02 * | 4.35 ± 0.03 | 3.65 ± 0.04 | 2.77 ± 0.01 * |

* apparent stability constants due to the heterogenous nature of the cyclodextrin

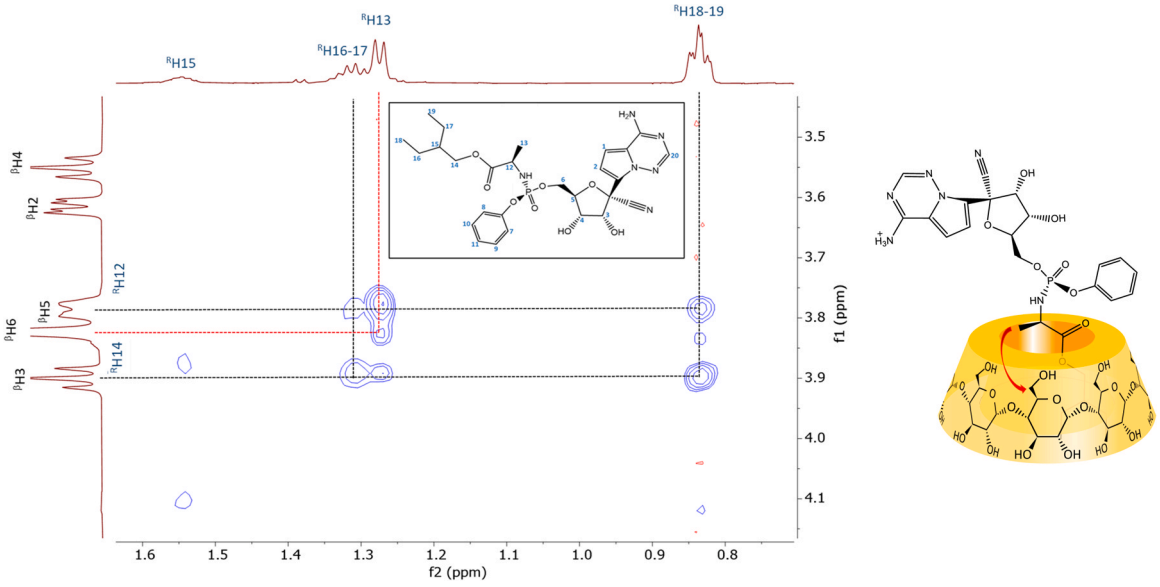


**Fig. 4.** Partial 2D ROESY spectrum of a 1:3 molar ratio (REM:βCD) sample and the structure of the suggested inclusion complex.

obtained stability constant indicates a much weaker intermolecular interactions compared to the permanently negatively charged CDs.

### 3.3. Structural characterization of REM-CD complexes by NMR

To obtain atomic-level information on the 3D structure of the complexes 2D ROESY NMR experiments were carried out at various host-guest molar ratios. In the case of βCD, 2D ROESY spectrum was registered on a 1:3 (REM:βCD) system in order to ensure significant excess of the host. A zoomed inset in Fig. 4 refers spatial proximities between the ethylbutyl-sidechain of REM and βCD. Intermolecular cross-peaks could be detected between the REM's methyl- (H18–19), the methylene- (H16-H17) and the inner cavity resonances of βCD (H3 and H5), proving that the aliphatic moiety immersed into the host cavity (Fig. 4). The encapsulation of alkyl chains is well-known in the literature, especially in the case of lipids [21]. As REM also possess a rather lipophilic phenoxy moiety too, its inclusion was also anticipated, however no inclusion of the phenoxy moiety was observed. There are literature examples where the immersion of branched alkyl sidechains is preferred even in the presence of an aromatic moiety [22].

The inclusion of the ethylbutyl-sidechain was also corroborated by a further interaction between the methyl resonance of the alanyl residue (H13) and the H6 methylene of the βCD, which unequivocally confirms that the inclusion occurs from the narrower rim of the CD (see Fig. 4).

The single isomeric nature and the concomitant simplicity of the NMR resonances of per-6-SBEβCD permitted the depiction of the spatial arrangement of REM-SBEβCD complex. The observed ROESY cross-peaks for the alanyl residue (H13) and the H6 resonances of per-6-SBEβCD assigned the direction of penetration of ethylbutyl-moiety of REM into the cavity from the primary side (see Supporting Information Fig. S18). Thus, the proposed arrangement allows the formation of electrostatic interactions between the CD's negatively charged sulfobutyl-sidechains and the REM's protonated heterocyclic moiety, thereby supporting the observed increase in complex stability. Our previous study [20] indicated, that the random substituted nature of SBEβCD makes difficult to determine the direction of REM's inclusion (Fig. S19), however SBEβCD possesses a random substituted nature, i.e. carries sulfobutyl-sidechains at position 2, 3 and 6 as well. Taking into consideration the identical inclusion mode for both βCD and per-6-SBEβCD along with the stability values, herein we propose that the SBEβCD-REM complex is also constructed in the same fashion (see Fig. 5).

The larger cavity of γCD is not perfectly suited for the ethylbutyl moiety, only weak intermolecular interactions could be observed in the 2D ROESY spectrum (see Supporting Information Fig. S20). However, clear evidences indicate that the phenoxy ring immerses into the cavity of γCD from its narrower side, supporting a weak interaction between γCD and REM (Fig. S20). The sulfobutylation of γCD resulted in stability enhancement, however, no conclusive complex structure could be derived due to broadened and diffuse NMR signals. In this case both aliphatic and aromatic parts of REM are involved in complexation (see Supporting Information Fig. S21). The single isomer γCD derivative sugammadex allowed a detailed NMR characterization of REM complexation at pH 2.0 (Supporting Information Fig. S22), where the most pronounced interaction was the immersion of the phenoxy moiety into the cavity from the wider rim (see Fig. 5.). Additionally, weak interactions could be deduced between the methyl resonances of ethylbutyl-sidechain and those of the cavity protons suggesting the co-existence of a different binding mode as shown in Fig. 5. Moreover, the ethylthio groups of sugammadex show spatial proximity with the aliphatic chain of REM (Fig. S22), however, this interaction lacks real inclusion of REM into the cavity. The intermolecular interaction is therefore established through the peripheral (ethylthio) groups of sugammadex and the alkyl sidechain of REM. Thus, REM complexation with sugammadex accommodates several geometries leading to a superior stability.

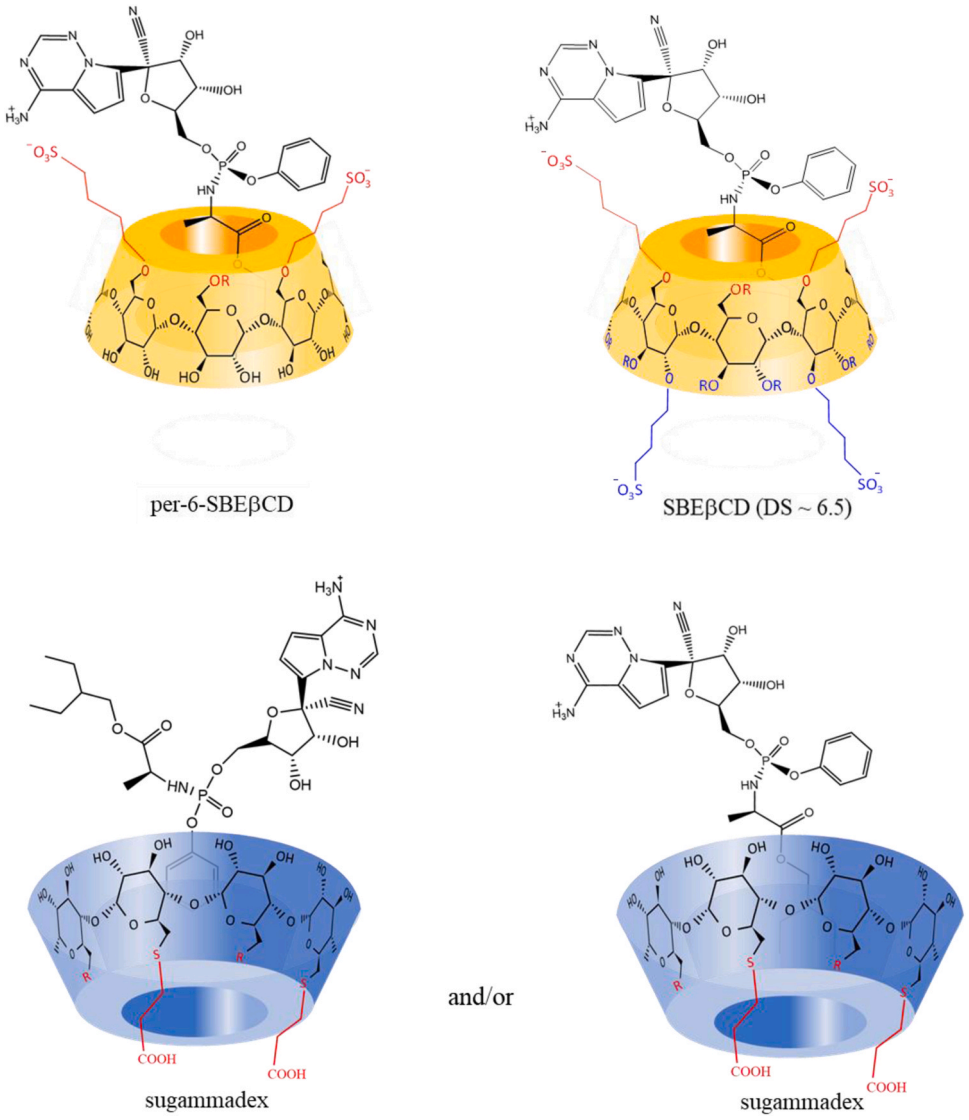


**Fig. 5.** Suggested structures of inclusion complexes of the two βCD derivatives (yellow) and REM and the proposed sugammadex-REM complexes (blue) based on 2D ROESY NMR spectra (under pH 2.0 conditions).

## 4. Conclusions

In the present study intermolecular interactions of REM and various CD derivatives were characterized extensively by NMR spectroscopy. The aim of this study was to understand in details the molecular-level interactions between REM and its excipient in Veklury™ (SBEβCD) and with other cyclodextrin derivatives. NMR spectroscopic studies revealed that introduction of the anionic sulfobutylether-sidechains on the CD hosts contributes to a significant stability enhancement, furthermore the primary side sulfobutylation of the host plays the most critical role in the stability of the inclusion complex. Possible complex structures were determined by 2D ROESY NMR experiments and revealed that mainly the ethylbutyl moiety is involved in the molecular encapsulation in REM-βCD systems. Besides, the inclusion of the phenoxy moiety was only observed in the case of γCD derivatives. In addition, the p$K_a$ value of REM was determined experimentally by UV-pH titration method here for the first time. The p$K_a$ value of the heterocyclic aminopyrrolo-triazin moiety yielded a p$K_a$ value of 3.56. Our results also highlighted that the charge state of the host and the guest may remarkably contribute to the inclusion complex formation of REM. As not only the formulation, but also the preparative scale purification and chiral analysis of REM poses several challenges for the analytical community our results may open the door of the application of cyclodextrins in those fields as well.

## Declaration of Competing Interest

The authors declare that they have no known competing financial interests or personal relationships that could have appeared to influence the work reported in this paper.

## Acknowledgments

B.V. thanks the financial support from the Semmelweis 250+ Ph.D. Excellence Scholarship (EFOP-3.6.3-VEKOP-16-2017-00009) and from the New National Excellence Program of the Ministry of Human Capacities (ÚNKP-21-3-I-SE-52). This work was partially supported by the János Bolyai Research Scholarship of the Hungarian Academy of Sciences and by the Bolyai+ New National Excellence Program (grant number: ÚNKP-20-5-SE-31) of the Ministry of Human Capacities.

## Appendix A. Supporting information

Supplementary data associated with this article can be found in the online version at doi:10.1016/j.jpba.2021.114482.

## References


[1] F. Wu, S. Zhao, B. Yu, Y.-M. Chen, W. Wang, Z.-G. Song, Y. Hu, Z.-W. Tao, J.-H. Tian, Y.-Y. Pei, M.-L. Yuan, Y.-L. Zhang, F.-H. Dai, Y. Liu, Q.-M. Wang, J.-J. Zheng, L. Xu, E.C. Holmes, Y.-Z. Zhang, A new coronavirus associated with human respiratory disease in China, Nature 2020 (2020) 265–269, https://doi.org/10.1038/s41586-020-2008-3

[2] P. Zhou, X.-L. Yang, X.-G. Wang, B. Hu, L. Zhang, W. Zhang, H.-R. Si, Y. Zhu, B. Li, C.-L. Huang, H.-D. Chen, J. Chen, Y. Luo, H. Guo, R.-D. Jiang, M.-Q. Liu, Y. Chen, X.-R. Shen, X. Wang, X.-S. Zheng, K. Zhao, Q.-J. Chen, F. Deng, L.-L. Liu, B. Yan, F.-X. Zhan, Y.-Y. Wang, G.-F. Xiao, Z.-L. Shi, A pneumonia outbreak associated with a new coronavirus of probable bat origin, Nature 2020 (2020) 270–273, https://doi.org/10.1038/s41586-020-2012-7

[3] Coronavirus (COVID-19) Update: FDA Issues Emergency Use Authorization for Potential COVID-19 Treatment | FDA, (n.d.). ⟨https://www.fda.gov/news-events/press-announcements/coronavirus-covid-19-update-fda-issues-emergency-use-authorization-potential-covid-19-treatment#:~:%7B%7D:text=The⟩ emergency use authorization allows,children hospitalized with severe disease (accessed July 14, 2021).

[4] T.K. Warren, R. Jordan, M.K. Lo, A.S. Ray, R.L. Mackman, V. Soloveva, D. Siegel, M. Perron, R. Bannister, H.C. Hui, N. Larson, R. Strickley, J. Wells, K.S. Stuthman, S.A. Van Tongeren, N.L. Garza, G. Donnelly, A.C. Shurtleff, C.J. Retterer, D. Gharaibeh, R. Zamani, T. Kenny, B.P. Eaton, E. Grimes, L.S. Welch, L. Gomba, C.L. Wilhelmsen, D.K. Nichols, J.E. Nuss, E.R. Nagle, J.R. Kugelman, G. Palacios, E. Doerffler, S. Neville, E. Carra, M.O. Clarke, L. Zhang, W. Lew, B. Ross, Q. Wang, K. Chun, L. Wolfe, D. Babusis, Y. Park, K.M. Stray, I. Trancheva, J.Y. Feng, O. Barauskas, Y. Xu, P. Wong, M.R. Braun, M. Flint, L.K. Mcmullan, S.-S. Chen, R. Fearns, S. Swaminathan, D.L. Mayers, C.F. Spiropoulou, W.A. Lee, S.T. Nichol, T. Cihlar, S. Bavari, Therapeutic efficacy of the small molecule GS-5734 against Ebola virus in rhesus monkeys, Nature (2016), https://doi.org/10.1038/nature17180

[5] R. Humeniuk, A. Mathias, H. Cao, A. Osinusi, G. Shen, E. Chng, J. Ling, A. Vu, P. German, Safety, tolerability, and pharmacokinetics of remdesivir, an antiviral for treatment of COVID-19, in healthy subjects, Clin. Transl. Sci. 13 (2020) 896–906, https://doi.org/10.1111/CTS.12840

[6] Y. chen Cao, Q. xin Deng, S. xue Dai, Remdesivir for severe acute respiratory syndrome coronavirus 2 causing COVID-19: an evaluation of the evidence, Travel Med. Infect. Dis. 35 (2020) 101647, https://doi.org/10.1016/J.TMAID.2020.101647

[7] Publication Classification ( 54) Compositions Comprising an Rna Polymerase Inhibitor and Cyclodextrin for Treating Viral, (2020).

[8] L. Szente, J. Szemán, Cyclodextrins in analytical chemistry: host-guest type molecular recognition, Anal. Chem. 85 (2013) 8024–8030, https://doi.org/10.1021/ac400639y

[9] L. Liu, Q.X. Guo, The driving forces in the inclusion complexation of cyclodextrins, J. Incl. Phenom. 42 (2002) 1–14, https://doi.org/10.1023/A:1014520830813

[10] M. Malanga, I. Fejős, E. Varga, G. Benkovics, A. Darcsi, J. Szemán, S. Béni, Synthesis, analytical characterization and capillary electrophoretic use of the single-isomer heptakis-(6-O-sulfobutyl)-beta-cyclodextrin, J. Chromatogr. A 1514 (2017) 127–133, https://doi.org/10.1016/J.CHROMA.2017.07.069

[11] K. Nag, D.R. Singh, A.N. Shetti, H. Kumar, T. Sivashanmugam, S. Parthasarathy, Sugammadex: a revolutionary drug in neuromuscular pharmacology, Anesth. Essays Res. 7 (2013) 302, https://doi.org/10.4103/0259-1162.123211

[12] Z. Szakács, B. Noszál, Determination of dissociation constants of folic acid, methotrexate, and other photolabile pteridines by pressure-assisted capillary electrophoresis, Electrophoresis 27 (2006) 3399–3409, https://doi.org/10.1002/elps.200600128

[13] S.H. Kamble, A. Sharma, T.I. King, F. León, C.R. McCurdy, B.A. Avery, Metabolite profiling and identification of enzymes responsible for the metabolism of mitragynine, the major alkaloid of Mitragyna speciosa (kratom), Xenobiotica 49 (2019) 1279–1288, https://doi.org/10.1080/00498254.2018.1552819

[14] D. Brynn Hibbert, P. Thordarson, The death of the Job plot, transparency, open science and online tools, uncertainty estimation methods and other developments in supramolecular chemistry data analysis, Chem. Commun. 52 (2016) 12792–12805, https://doi.org/10.1039/c6cc03888c

[15] L. Fielding, Determination of association constants (K(a)) from solution NMR data, Tetrahedron 56 (2000) 6151–6170, https://doi.org/10.1016/S0040-4020(00)00492-0

[16] S. Krait, A. Salgado, B. Chankvetadze, F. Gago, G.K.E. Scriba, Investigation of the complexation between cyclodextrins and medetomidine enantiomers by capillary electrophoresis, NMR spectroscopy and molecular modeling, J. Chromatogr. A 1567 (2018) 198–210, https://doi.org/10.1016/j.chroma.2018.06.010

[17] A. Artese, V. Svicher, G. Costa, R. Salpini, V.C. Di Maio, M. Alkhatib, F.A. Ambrosio, M.M. Santoro, Y.G. Assaraf, S. Alcaro, F. Ceccherini-Silberstein, Current status of antivirals and druggable targets of SARS CoV-2 and other human pathogenic coronaviruses, Drug Resist. Updat. 53 (2020), https://doi.org/10.1016/j.drup.2020.100721

[18] W. Bray, Covid-19 Clarification of the remdesivir bonding model; remdesivir mechanism validates 2-phosphonobenzoic acid polymerase total inhibition, (2020). https://doi.org/10.13140/RG.2.2.18663.88484.

[19] W. Al-Soufi, P.R. Cabrer, A. Jover, R.M. Budal, J.V. Tato, Determination of second-order association constants by global analysis of 1H and 13C NMR chemical shifts, Steroids 68 (2003) 43–53, https://doi.org/10.1016/s0039-128x(02)00114-9

[20] L. Szente, I. Puskás, T. Sohajda, E. Varga, P. Vass, Z.K. Nagy, A. Farkas, B. Várnai, S. Béni, E. Hazai, Sulfobutylether-beta-cyclodextrin-enabled antiviral remdesivir: characterization of electrospun- and lyophilized formulations, Carbohydr. Polym. 264 (2021) 118011, https://doi.org/10.1016/J.CARBPOL.2021.118011

[21] L. Szente, É. Fenyvesi, Cyclodextrin-Lipid complexes: cavity size matters, Struct. Chem. 2016 (2016) 479–492, https://doi.org/10.1007/S11224-016-0884-9

[22] S. Béni, T. Sohajda, G. Neumajer, R. Iványi, L. Szente, B. Noszál, Separation and characterization of modified pregabalins in terms of cyclodextrin complexation, using capillary electrophoresis and nuclear magnetic resonance, J. Pharm. Biomed. Anal. 51 (2010) 842–852, https://doi.org/10.1016/J.JPBA.2009.10.010